This is the Pre-Published Version.

Field Computation and Performance of a Series-Connected Self-Excited Synchronous Generator

T. F. Chan[1], Weimin Wang[1], and Loi Lei Lai[2]
[1]Department of EE, The Hong Kong Polytechnic University, Hung Hom, Hong Kong, China
[2]Energy Systems Group, School of Engineering and Mathematical Sciences, City University London, UK
eetfchan@polyu.edu.hk

***Abstract* — This paper presents the field computation and the operating characteristics of a series-connected self-excited synchronous generator. Modeling for time-stepping coupled field –circuit analysis is explained. A detailed study on the self-excitation phenomenon and load performance is presented. The proposed analysis is vigorously tested on a three-phase, 1.8-kW slip-ring induction machine for various operating conditions. The computed results obtained by the FEA are found to be in good agreement with experimental results.**

I. INTRODUCTION

A series-connected self-excited synchronous generator (SCSESG) is a wound-rotor induction machine in which the stator and rotor windings are connected in series, the phase sequences of the stator being opposite to that of the rotor [1]-[4]. Fig. 1 shows the circuit arrangement of the generator. When driven by an external prime mover and a suitable capacitance is connected across the stator terminals, the machine will self-excite and deliver electrical power at a frequency equal to half of the rotor angular frequency. A high energy density and a large power output can be achieved as both the stator and rotor windings are involved in the energy conversion process. A typical application is as a high-speed wind turbine generator for distributed generation [1]. Steady-state and transient D-Q theory have been used for analyzing this type of machine [2]-[4]. Performance of this type of machine based on field analysis, however, has not been attempted before. In this paper, we briefly address the field computation aspects with reference to the SCSESG and then, we present a comparison between the experimental and computed results based on two-dimensional finite element analysis (2-D FEA) in order to verify the feasibility of the proposed approach. The experimental machine chosen for the present study is a 1.8 kW, four-pole, 50 Hz three-phase slip-ring induction machine with technical details listed in Table I.

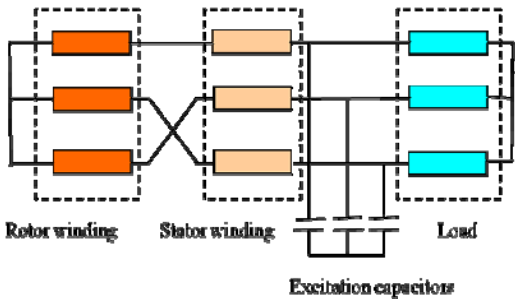

Fig. 1. Circuit connection of SCSESG

II. COMPUTATION METHOD

In order to simulate the operating conditions of the SCSESG the electromagnetic field computation method has adopted the following features:

- Due to the existence of magnetic circuits with saturated magnetic materials a nonlinear FEA is adopted.
- The anti-periodic boundary condition is applied to the field analysis to decrease computation time.
- Time-stepping FEM is employed in order to evaluate the transient characteristic of the generator voltage and current due to self excitation phenomenon and rotor movement.

A. Governing Equations

The governing system of equations for 2-D FEA is derived from Maxwell's equations [5]

$$\nabla \times (\nu \nabla \times A) - \nabla \nu_e \nabla \cdot A = -\sigma \tfrac{\partial A}{\partial t} - \sigma \nabla V \qquad (1)$$

where A is the magnetic vector potential, ν is the reluctivity tensor, σ is the conductivity tensor, and ν_e is defined as one third of the trace of reluctivity tensor. In the analysis, the winding is assumed to be composed of stranded coils, each having many fine turns in series and with eddy current effect ignored. For a stranded coil, (1) becomes:

$$\nabla \times (\nu \nabla \times A) - \nabla \nu_e \nabla \cdot A = J \qquad (2)$$

with the current density given by

$$J = i_n \tfrac{n}{S_c} i(t). \qquad (3)$$

where S_c is the coil cross-sectional area, n is the number of turns and $i(t)$ is the current per turn. i_n is a unit vector to indicate that the coil current is in the z (axial) direction.

Note that with 2-D analysis, the second term on the left of (1) and (2) will vanish.

B. Field Modeling and Field-Circuit Coupling with Periodic Boundary Condition

Fig. 2 shows the FE mesh of a quarter cross-section of the experimental SCSESG. To realize time-stepping, the slip surface of stator air gap and rotor air gap is each divided into 90 elements, which implies that a time step of 2 electrical degrees is used. Quadrilateral-shaped elements are used for meshing in order to improve the computational accuracy and to save computation time.

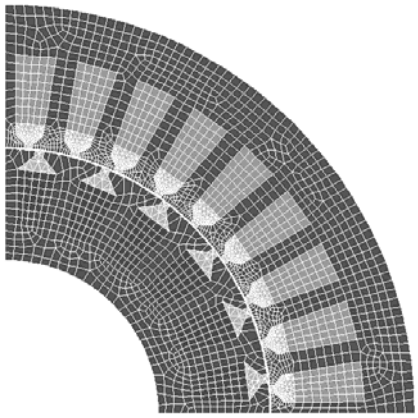

Fig. 2. Mesh of the SCSESG model

Modeling of the external electric circuit is achieved by using the connectivity patterns between various circuit elements such as resistors, capacitor and inductors. Such elements consist of nodes having voltage potential DOF (degree of freedom). The nodes of the stranded coils possess magnetic potential A_z, EMF and current DOFs in the field region. The stranded coil represents a current source in the circuit loop, and it has three nodes. Two nodes carry the voltage potential DOF and these are used for connection with other circuit elements; the third node is any node in the field region for the stranded coil, and this latter node carries current and EMF information. Since anti-periodic boundary condition is applied to the field region, the current source for the conductor regions in the remaining ¾ of the machine cross-section can be directly coupled to the nodes of the conductors within the field region being modeled.

The external circuit consists of the coil-sides that make up the stator and rotor windings, together with the lumped stator and rotor resistances and leakage inductances, the excitation capacitances, and the load impedances. In the FEA model used, the total number of field variables is 9590 and the total number of circuit variables is 92 (which are due to the circuit nodes as well as the nodes linked to the slot conductor regions). There are thus a total of 9682 field-circuit variables.

C. Initial Conditions for Field Computation

Modeling of the residual flux in the FEA computation presents some difficulties as the residual flux cannot be easily incorporated into the material properties in the machine model. To overcome this problem the initial current is specified instead. Computations showed that both the initial current DOF value for the conductor region and initial voltage potential set up for terminals are important for successful simulation of voltage build up.

It was found that the residual current magnitude should be about 0.15A to initiate voltage build-up. The proper phase of the electrical angle can be estimated from the relationship between stator and rotor MMFs under steady-state conditions [3]. Under no-load or medium load conditions, a phase angle of -11.2 electrical degrees was found to yield satisfactory computed results.

At the start of the time-stepping FEA, it was necessary to set the voltage potential of three stator phase terminals to 0 V. The voltage DOF constraint should be deleted after the initial time step computation.

III. RESULTS

A. Field Computation Results

The stator end-winding leakage inductance L_{es} of the prototype SCSESG is 0.154 mH, and the rotor end-winding leakage inductance L_{er} is 0.025 mH, determined using an analytical method [6]. It is also assumed that both the stator and rotor cores are made of M36-26G iron material. A frontal direct equation solver [7], which minimizes the memory used in the solution process, is chosen for the analysis. There are 9682 unknowns in the FE model, and computation for each load condition is 720 to ensure steady-state is reached. On a Sun Microsystems Sun-fire E6900 CPU 4 x 900 MHz 64 bits processor memory 4GB the total computation time for a typical analysis of transient voltage build-up is approximately 6.5 h.

Fig. 3 shows the computed no-load flux line distribution for a rotor position of 60 electrical degrees when C = 120 μF and the rotor speed is 1500 r/min. Fig. 4 shows the computed radial flux density distribution for the same rotor position when the generator is under no load and when supplying a resistive load of 131.7 Ω per phase, respectively. It can be seen that the air gap flux density decreases when the generator is loaded, which implies that the terminal voltage will decrease. The results also indicate that the air gap flux density has substantial ripple contents due to the stator and rotor slot openings. Fig. 5 shows the voltage across an 11-turn full-pitched search coil when C = 120 μF and the rotor speed is 1500 r/min, the SCSESG being under no-load condition. The rich ripple content of the search coil voltage waveform to a certain extent confirms the computed results of air gap flux density as shown in Fig. 3.

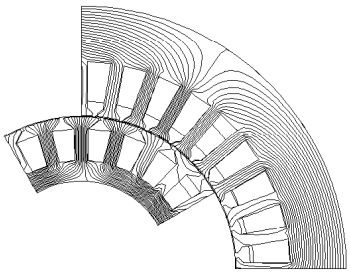

Fig. 3. Computed flux line distribution at a rotor position of 60 electrical degrees under no load condition (C=120 μF, speed = 1500 rpm)

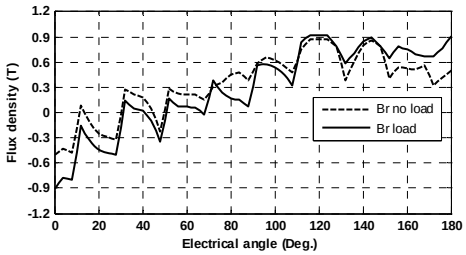

Fig. 4. Computed radial flux density distribution at a rotor position of 60 electrical degrees under no load and loaded conditions (C=120 μF, speed = 1500 r/min)

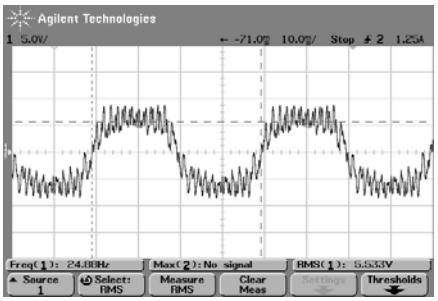

Fig. 5. Measured voltage across an 11-turn, full-pitched search coil in stator slots (C = 120 μF, speed = 1500 r/min)

B. *Voltage Build-up*

Fig. 6 shows the computed no-load line voltage build-up process when C = 120 μF and the rotor speed is 1428 r/min, The initial current magnitude was chosen as 0.15 A in order to account for the remanent flux of SCSESG. This is verified by the experimental waveform of transient voltage build-up under the same conditions as shown in Fig. 7. It is observed that the SCSESG has an extremely short period of transient voltage build up, steady-state voltage being reached in about 5 cycles, or 250 ms. Fig. 8 shows the voltage build up with different initial current magnitudes under no-load condition. A large initial current magnitude results in a more vigorous transient build-up, but as time passes the steady-state voltage becomes the same. Computations also show that the time for voltage build-up increases when the excitation capacitance is larger and a higher steady-state output voltage is obtained.

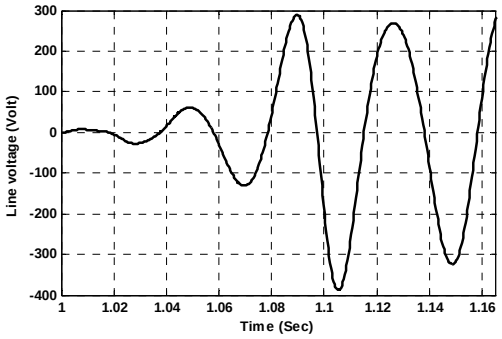

Fig. 6. Computed voltage build up of SCSESG under no-load condition (C=120 μF, speed = 1428 r/min)

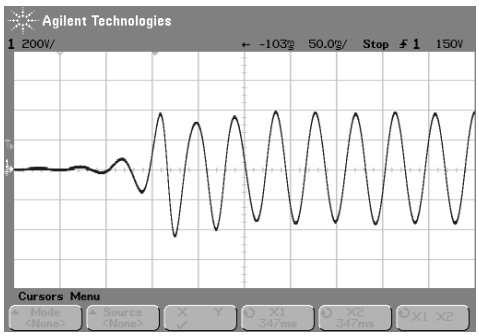

Fig. 7. Measured voltage build up of SCSESG under no-load condition Voltage scale: 200 V/div; time scale: 50 ms/div (C=120 μF, speed = 1428 r/min)

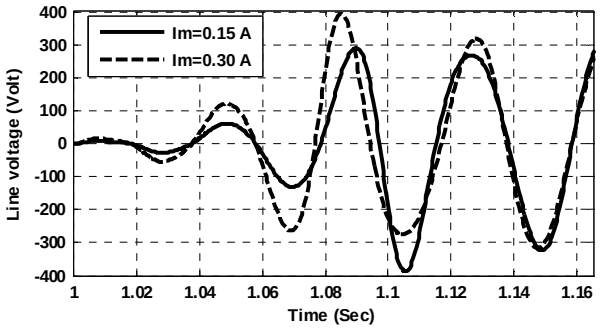

Fig. 8. Computed voltage build up with different initial current magnitudes under no-load condition (C=120 μF, speed = 1428 r/min)

C. *Steady-State Performance*

Fig. 9 shows the computed no-load stator and rotor phase voltages when C = 120 μF and the rotor speed is 1500 r/min. It is observed that both the stator and rotor phase voltages contain appreciable slot ripples, as predicted from the computed air gap flux density waveforms in Fig. 3. Fig. 10 shows the computed no-load three-phase line voltage and capacitor current under the same conditions. Unlike the phase voltages, both the line voltages and capacitor currents are almost sinusoidal. The series connection of the stator and rotor windings thus results in cancellation of slot ripples in the output line voltage.

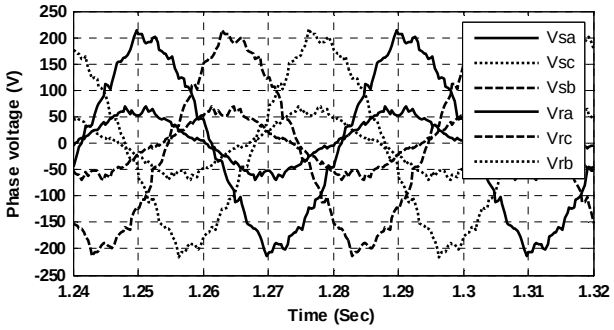

Fig. 9. Computed stator and rotor phase voltage under no-load condition (C=120 μF, speed = 1500 r/min)

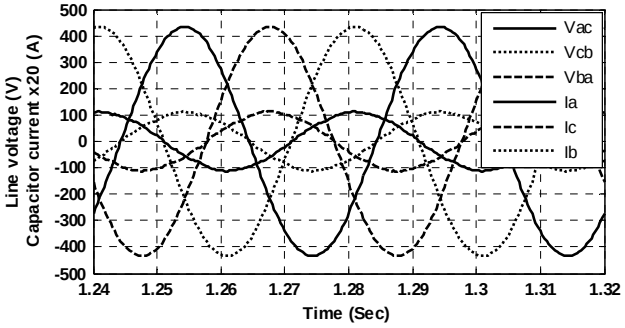

Fig. 10. Computed line voltage and capacitor current under no-load condition (C=120 μF, speed = 1500 r/min)

D. *Performance Characteristics*

Fig. 11 shows the computed and measured no-load voltage versus speed when the excitation capacitance is 120 μF, 200

μF and 280 μF. It can be observed that the voltage increases with generator speed, and higher voltages are produced by a larger capacitance. For a given capacitance, the SCSESG cannot maintain the excitation below a certain cutoff speed. The load characteristic of the SCSESG is shown in Fig. 12. A reasonably good agreement between computed and experimental results is observed, the discrepancies being due to the difficulty in obtaining an accurate magnetization curve of the slip-ring machine.

The experimental results in Fig. 14 and 15 further confirm the waveforms of the SCSESG predicted by time-stepping FEA.

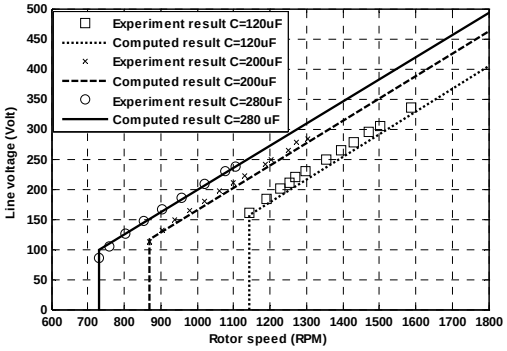

Fig. 11. Variation of no-load voltage of SCSESG with speed

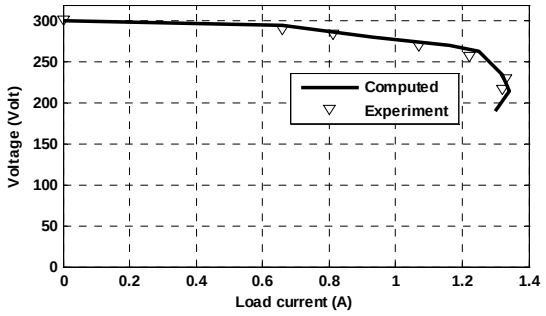

Fig. 12. Computed and experimental load characteristics at a speed of 1500 r/min when C = 120 μF

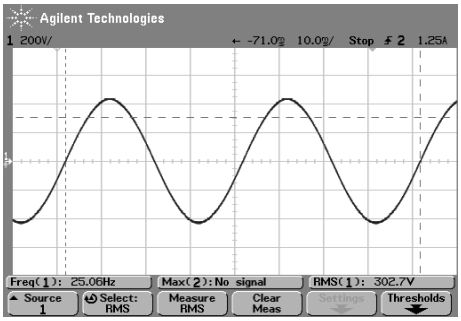

Fig. 13. No-load terminal line voltage waveform of SCSESG
Voltage scale: 200 V/div; time scale: 10 ms/div
(C=120 μF, speed = 1500 r/min)

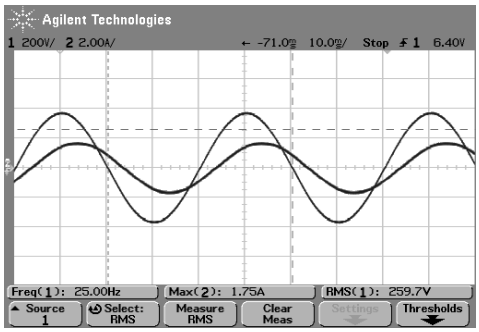

Fig. 14. Waveforms of terminal line voltage and load current when SCSESG is delivering a current of 1.15 A to a balanced resistive load
Voltage scale: 200 V/div; current scale: 2 A/div; time scale: 10 ms/div
(C=120 μF, speed = 1500 r/min)

TABLE I
WINDING DETAILS OF EXPERIMENTAL SCSESG

	Stator	Rotor
Rated current	4.5 A	10 A
Number of slots per pole	9	6
Type of winding	Single layer, concentric	Single layer, full pitch
Turns per coil	48	24
Resistance per phase	2.6 Ω	0.59 Ω
Leakage inductance per phase	0.154 mH	0.025 mH

IV. ACKNOWLEDGMENT

The work described in this paper was fully supported by the Hong Kong Polytechnic University under grant G-U487.

V. REFERENCES

[1] Tze-Fun Chan and Loi Lei Lai, "Use of the slip-ring induction machine for distributed generation," in *Proc. IEEE Power and Energy Society General Meeting*, 20-24 Jul. 2008, Pittsburg, PA, USA

[2] A. L. Mohamadein, H. A.Yousef and Y. G. Dessouky, "Series-connected self-excited synchronous generator: steady state and transient behaviors", *IEEE Trans. Energy Convers.*, 14(4): 1108-111, 1999.

[3] A. L. Mohamadein and E. A. Shehata, "Theory and performance of series connected self-excited synchronous generators", *IEEE Trans. Energy Convers.*, 10(3): 508-515, 1995.

[4] A. S. Mostafa, A. L. Mohamadein and E. M. Rashad, "Analysis of series-connected wound-rotor self-excited induction generators", *IEE Proceedings Electric Power Applications*, 140(5): 329-336, 1993.

[5] Jianshe Wang, "A nodal analysis approach for 2D and 3D magnetic-circuit coupled problems," *IEEE Trans. Magnetics*, 32(3): 1074-1077, 1996.

[6] J. F. Gieras, *Permanent-Magnet Motor Technology,* 2rd ed., Marcel Dekker: New York, 2002.

[7] B. M. Irons, "A Frontal Solution Program for Finite Element Analysis", *International Journal for Numerical Methods in Engineering*, 2(1): 5-23. Jan. 1970.